

**On robustness against JPEG2000: a performance
evaluation of wavelet-based watermarking techniques**

BHOWMIK, Deepayan <<http://orcid.org/0000-0003-1762-1578>> and
ABHAYARATNE, Charith

Available from Sheffield Hallam University Research Archive (SHURA) at:

<https://shura.shu.ac.uk/14107/>

This document is the Accepted Version [AM]

Citation:

BHOWMIK, Deepayan and ABHAYARATNE, Charith (2014). On robustness against
JPEG2000: a performance evaluation of wavelet-based watermarking techniques.
Multimedia Systems, 20 (2), 239-252. [Article]

Copyright and re-use policy

See <http://shura.shu.ac.uk/information.html>

On robustness against JPEG2000: A performance evaluation of wavelet-based watermarking techniques

Deepayan Bhowmik · Charith Abhayaratne

Received: 01-Sept-2012 / Accepted: date

Abstract With the emergence of new scalable coding standards, such as JPEG2000, multimedia is stored as scalable coded bit streams that may be adapted to cater network, device and usage preferences in multimedia usage chains providing universal multimedia access. These adaptations include quality, resolution, frame rate and region of interest scalability and achieved by discarding least significant parts of the bit stream according to the scalability criteria. Such content adaptations may also effect the content protection data, such as watermarks, hidden in the original content. Many wavelet-based robust watermarking techniques robust to such JPEG2000 compression attacks are proposed in the literature. In this paper, we have categorized and evaluated the robustness of such wavelet based image watermarking techniques against JPEG2000 compression, in terms of algorithmic choices, wavelet kernel selection, subband selection, or watermark selection using a new modular framework. As most of the algorithms uses a different set of parametric combination, this analysis is particularly useful to understand the effect of various parameters on the robustness under a common platform and helpful to design any such new algorithm. The analysis also considers the imperceptibility performance of the watermark embedding, as robustness and imperceptibility are two main watermarking properties, complementary to each other.

Keywords Wavelet-based image watermarking · watermarking evaluation · robustness · scalable coding · content adaptation · JPEG2000

1 Introduction

Recent years have seen the emergence of scalable coding standards for multimedia content coding: JPEG2000 for images [1]; MPEG advanced video coding (AVC)/H.264 scalable video coding (SVC) extension for video [2]; and MPEG-4 scalable profile for audio [3]. The scalable coders produce scalable bit streams representing content in hierarchical layers according to audiovisual quality, spatio-temporal resolutions and regions-of-interests. The bit streams may be accordingly truncated in order to satisfy variable network data rates, display resolutions, display device resources and usage preferences. The new bit streams may be transmitted or further adapted or decoded using a universal decoder which is capable of decoding any original or adapted bit streams to display or play adapted versions of the original content in terms of quality or reductions. The multimedia usage framework standard, MPEG-21, standardizes the operation of a content-agnostic content adaptation engine as the part 7 of the standard: Digital Item Adaptation (DIA) [4, 5]. Such bit stream truncation-based content adaptations also affect any content protection data, such as watermarks, embedded in the original content. In this paper, we consider JPEG2000 compression as the scalable coding-based content adaptations for images. Therefore JPEG2000 based attacks are considered here as an important potential attack on the watermarking schemes.

Due to the use of digital wavelet transform (DWT) as the underlying technology of JPEG2000 compression standard, recent years have seen wide use of wavelet-based techniques for image watermarking [6–32] in order to improve the watermarking robustness. However, these algorithms are often different to each other in terms of the wavelet kernel, number of wavelet decomposition levels, wavelet sub band choices for embedding, wavelet coefficient choices for embedding and the coefficient modification method for embedding. Therefore it is extremely difficult to evaluate such algorithms when comparing the performances. Often the algorithms claim improvements compared to the previously proposed ones but offer very little information on the reason behind it. Literature suggest that often wavelet kernels [24, 33] or a hosting coefficient selection method [6, 7, 17, 22] may play a key role in watermarking performance while it is very difficult to understand whether the improvements are influenced by any other parametric choices or not. For example, while it is general convention that high-frequency sub-band based watermarking offer high imperceptibility and less robustness to compression. However literature [34] proposed that not all high frequency coefficients are vulnerable to compression while not all low frequency coefficients are robust to compression. In this case the performance evaluation with any other existing method is very difficult unless compared under a common platform. Therefore it is important to study the effect of previously mentioned parametric choices in terms of balanced embedded distortion and robustness to content adaptation attacks performances under a common framework. Such framework is particularly helpful to help the reader to choose various design parameters in proposing a new watermarking algorithm. Subsequent sections of this paper discussed in details about such parametric dissection of these algorithms.

The main aim of this paper is to address the evaluation of wavelet-based image watermarking schemes for robustness against scalable coding-based content adaptation attacks, *e.g.*, JPEG2000 by proposing a new analysis framework. However, the paper also considers another important requirement of watermarking, the im-

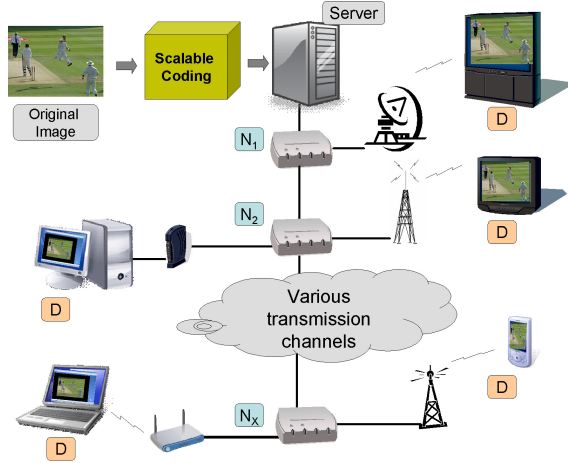


Fig. 1 Universal multimedia usage scenarios using scalable coded content.

perceptibility, which is often complementary in nature to robustness. For example, in order to lower the embedding distortion, one may choose low significant frequencies or low significant bit plane which often forms the low significant portions of the scalable bit streams which may be discarded during content adaptations. In summary, the main objectives of this paper are:

1. To categorize and dissect wavelet-based image watermarking schemes under one common platform.
2. To design a new framework to analyze the effects of various algorithmic parameters on robustness.
3. To evaluate the robustness of wavelet-based image watermarking techniques against JPEG2000 scalable content adaptations.

The rest of the paper is organized as follows: General overviews of scalable coding-based content adaptation is presented in Sect. 2 followed by the detailed dissection of the wavelet-based watermarking techniques in Sect. 3. The new evaluation framework is presented in Sect. 4, whereas the evaluation results are discussed in Sect. 5 followed by concluding remarks in Sect. 6.

2 Overview of scalable coding-based content adaptation

The universal media access (UMA) is an important requirement in modern multimedia usage chains. The UMA concept envisages seamless delivery of multimedia across heterogeneous networks and various devices. This would require catering for different network bandwidths, transmission media, device capabilities, memory and power availability and most importantly usage preferences. This can only be achieved by intelligent content-agnostic adaptations based on the scalable coded content representations. An example of scalable coding-based multimedia usage is shown in Fig. 1. In scalable coding the input media is coded in a way that the main host server keeps bit streams that can be decodeable to high quality full resolution content. When the content needs to be delivered to a less capable display

or via a lower bandwidth network, the bit stream is adapted at different nodes (N_1, N_2, \dots, N_x , as shown in Fig. 1) using different scaling parameters to match those requirements. At each node the adaptation parameters may be different and a new bit stream may be generated. Finally the adapted bit streams are decoded using a universal decoder. The scalable coding-decoding process consists of 3 main modules [35]: encoder, extractor and decoder.

The **encoder module** is responsible for producing a full resolution, highest quality compressed bit stream from the original content. The bit stream generation normally focuses on three main functionalities: quality scalability (Q_i), spatial resolution scalability (S_i) and temporal resolution scalability (T_i : for video), where Q_i , S_i and T_i represent the scaling parameters for different quality-spatio-temporal layers with the layer index i . A bit stream descriptor is also generated along with the bit stream describing the location of these layers in the scalable bit stream.

The **extractor module** is part of a cross media engine that adapts the bit streams following the MPEG 21 part-7 DIA specifications. It truncates the scalable bit stream considering the context and produces the adapted bit-stream, which is also scalable and can be re-adapted at any following network node by using another extractor, and its new description.

The **decoder module** provides an universal decoder to decode any adapted bitstream to display the adapted content.

3 Wavelet-based image watermarking

Due to its ability for efficient multi-resolution spatio-frequency representation of signals, the DWT has become the major transform for spread spectrum watermarking. The wavelet domain watermarking algorithms often share a common model. Based on the embedding methodology, wavelet-based image watermarking can be categorized into two main classes: uncompressed domain algorithms and joint compression-watermarking algorithms.

Uncompressed domain watermarking algorithms: Watermark embedding is performed independent of and prior to compression. There are many algorithms of this type of watermarking, presented in the literature [6–9, 11–14, 17–20, 22–24]. A system block diagram in the context of scalable coding-based content adaptation is shown in Fig. 2. The major steps for embedding include the forward DWT (FDWT) and coefficient modification followed by the inverse DWT (IDWT). Then the content is scalable coded and may be adapted during usage. Watermark authentication includes the FDWT and recovery of the watermark as blind or non-blind extraction and comparison with the original watermark.

Joint compression-watermarking algorithms: As scalable image coding is mainly based on the DWT, joint compression-watermarking algorithms [25–28, 30–32] incorporated into JPEG2000 are also becoming more efficient way of image watermarking. A general system block diagram is shown in Fig. 3. In most cases the watermark is embedded by modifying the quantized wavelet coefficients and the watermark is extracted during image decoding. It is worth to note that the embedding DWT kernel and the compression DWT kernel are same in this case. The use of JPEG2000 lossless mode in this category resembles to an uncompressed-domain

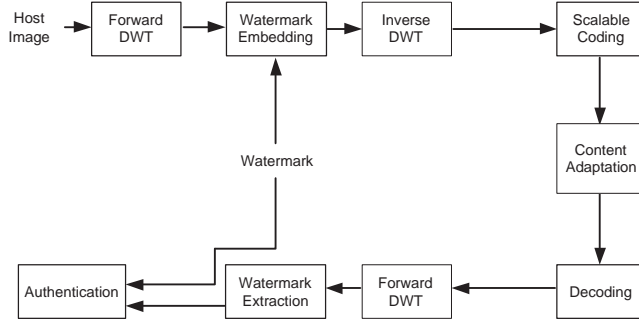


Fig. 2 Uncompressed domain image watermarking and content adaptation attack.

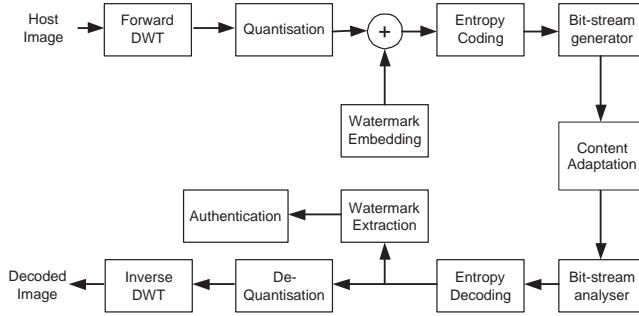


Fig. 3 Joint compression-watermarking and content adaptation attack.

watermarking algorithm that uses the same DWT kernel for both compression and watermark embedding.

3.1 Dissection of wavelet-based image watermarking algorithms

In both algorithm types, the watermark embedding algorithm considers different options for the choice of wavelet kernels, embedding subbands, for the selection of embedding coefficients and the modification methodology. In this section we dissect the well-known wavelet-based algorithms in terms of these four parameters:

3.1.1 Wavelet kernel

Early work on wavelet-based watermarking used mainly Haar or other Daubechies family orthogonal wavelets [6–9, 11–15, 17–19]. Then with the success of biorthogonal wavelets in image coding, they have been used in watermarking algorithms [22–24, 29]. Further, joint compression-watermarking algorithms are also considered as biorthogonal wavelet domain watermarking. With the introduction of lifting-based wavelet design, lifting-based integer-to-integer Haar transform [8, 21] and lifting-based non-linear wavelets [22] have been used in watermarking algorithms. A more comprehensive study on the use of various wavelet kernels in watermarking algorithms can be found at [33, 36, 37].

3.1.2 Subband

Often various watermarking algorithms select different number of wavelet decomposition levels to choose a desired subband or combination of subbands to suit algorithmic needs. There have been algorithms using two [6–9, 11], three [15, 22–24] and four [13, 14, 19] levels of wavelet decompositions. Joint compression-watermarking algorithms used the same number of levels of decompositions used in the compression algorithm. The choice of subbands for watermark embedding is often driven by the imperceptibility and robustness criteria. Algorithms intending to meet low embedding distortion and imperceptibility requirements use high frequency subbands for embedding [7–9, 11–14, 17, 28]. On the other hand, algorithms designed to achieve high robustness against compression use low frequency subbands for embedding [6, 16, 19, 22]. Finally, algorithms aiming to meet a balance between these two criteria use all subbands resulting in spread spectrum embedding [23–26].

3.1.3 Hosting coefficient

The selection of wavelet coefficients to host the watermark can be classified into three methods: choosing all coefficients in a subband [9, 11–14, 25, 31]; using a threshold based on their magnitude significance [8, 23, 24, 28] or the just noticeable difference (JND) [22]; and based on the median of a 3x1 non-overlapping window, which can be based on the same subband (Intra-band) [6, 26] or spanning three high frequency subbands in the same decomposition level (Inter-band) [7, 17]. Some of the all-coefficients-based algorithms use a Human Visual System (HVS)-based mask [12, 13] or a fusion rule-based mask for refining the selection of host coefficients [14, 15] or key-based random sequence for ordering host coefficients [19].

3.1.4 Embedding method

The host wavelet coefficient modification methods used in wavelet-based watermarking algorithms can be generalized as follows:

$$C'_{m,n} = C_{m,n} + \Delta_{m,n}, \quad (1)$$

where $C'_{m,n}$ and $C_{m,n}$ are the modified and original coefficients, respectively at (m, n) position, and $\Delta_{m,n}$ is the embedding modification. The modification methods can be categorized into two classes: modification based on magnitude alteration [8, 9, 11–15, 22–25, 28, 31]; and re-quantization of a coefficient with respect to a group of coefficients within a given window [6, 7, 17, 19, 26].

Further, for magnitude alteration algorithms, the way $\Delta_{m,n}$ in Eq. (1) is modified can be mapped into a generalized form consisting of four sub-classes of methods as follows:

$$\Delta_{m,n} = a_1 A_1 + a_2 A_2 + a_3 A_3 + a_4 A_4, \quad (2)$$

where

$$A_1 = \alpha C_{m,n}^b W_{m,n},$$

$$A_2 = v_{m,n} W_{m,n},$$

$$A_3 = \beta_{m,n} w_{m,n} \text{ and}$$

$$A_4 = f(C_{m,n}, W_{m,n}).$$

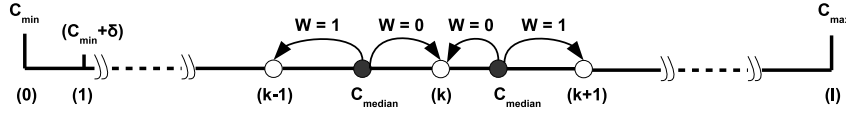


Fig. 4 Re-quantisation-based modification.

A_1 corresponds to direct modification of the host coefficient $C_{m,n}$ with a watermark value $W_{m,n}$ according to the user specified parameters (α and $b = 1, 2, \dots$) to vary the watermark weight and the strength, respectively [9, 22–25]. A_2 corresponds to the HVS driven modification using a weighting parameter ($v_{m,n}$) which is a function of $C_{m,n}$ and the pixel masking process in the HVS model [12, 13, 28]. A_3 corresponds to fusion-based methods where the host wavelet coefficients are fused with the watermark wavelet coefficients $w_{m,n}$ using an HVS-based fusion strength parameter, $\beta_{m,n}$ [14, 15]. With A_4 , we represent all other magnitude alteration algorithms based on any function, $f(C_{m,n}, W_{m,n})$. It is worth to mention that at a time only one type of modifications in Eq. (2) is used to represent individual algorithms and also used for experimental evaluation in Sect. 5. Therefore, we use a binary vector $\langle a_1, a_2, a_3, a_4 \rangle$ to represent specific algorithm by setting the corresponding vector element to 1 in the evaluation framework. The use of this vector is prominent in the next section.

Similarly we map the re-quantization-based modification into Eq. (1) as follows: Such algorithms change the median coefficient of a group of coefficients to the k^{th} quantisation step position by a modification value $\Delta_{m,n}$, where $|\Delta_{m,n}| \leq \delta$, which is based on the new quantization step δ as shown in Fig. 4. Different functions are suggested in the literature to find the value of δ and such functions normally use the minimum (C_{min}) and the maximum (C_{max}) coefficient values in the coefficients group. They can be generalized into the following form:

$$\delta = f(\gamma, C_{min}, C_{max}), \quad (3)$$

where γ is the user defined weighting factor. As $\Delta_{m,n}$ depends on the step size δ and the user defined γ , the modification value $\Delta_{m,n}$ is typically a function of C_{min} and C_{max} for each group of coefficients. Details of the embedding procedures can be found in [6] and [17].

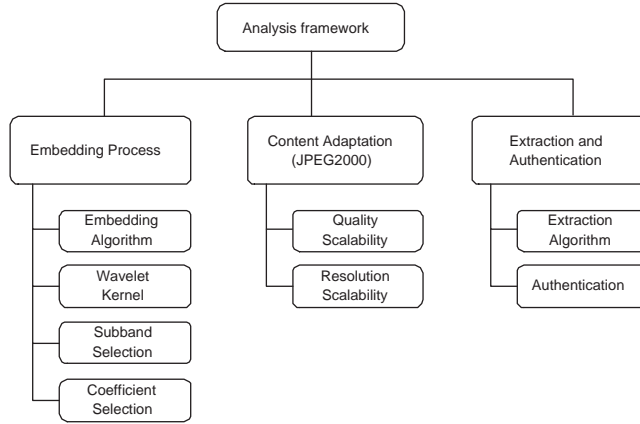
3.2 Different wavelet-based watermarking algorithm realization

With the above dissection, different wavelet-based watermarking algorithms can be realized under a common framework, based on various parametric options such as, the wavelet kernel, wavelet decomposition, subband choice, host coefficient choice and embedding method, and using a set of user-defined parameters. A examples of realization of major wavelet-based watermarking algorithms are shown in TABLE 1.

We use the above parametric dissection of state-of-the-art wavelet-based watermarking algorithms, in designing a new framework to evaluate the effects of these parameters on the robustness against JPEG2000.

Table 1 Realization of major wavelet-based watermarking algorithms using parametric dissection

Wavelet Kernel	Decom-position Levels	Sub band	Host Coefficient Selection	Embedding Method Choice	The Resulting Algorithm
Orthogonal	2	Low	Median	Intra Re-quantization	[6]
Orthogonal	2	High	Median	Inter Re-quantization	[7]
Orthogonal	2	High	Threshold	$\langle 1, 0, 0, 0 \rangle (b = 1)$	[8]
Haar	2	High	All	$\langle 1, 0, 0, 0 \rangle (b = 2)$	[9]
Orthogonal	2	High	All	$\langle 0, 0, 0, 1 \rangle$	[11]
Orthogonal	3	High	All	$\langle 0, 1, 0, 0 \rangle$	[12]
Orthogonal	4	High	HVS	$\langle 0, 1, 0, 0 \rangle$	[13]
Orthogonal	4	High	Fusion rule	$\langle 0, 0, 1, 0 \rangle$	[14]
Orthogonal	3	All	Fusion rule	$\langle 0, 0, 1, 0 \rangle$	[15]
Haar	2	Low	All	Intra Re-quantization	[16]
Haar	1	High	Median	Inter Re-quantization	[17]
Orthogonal	4	Low	Key based random sequence	Intra Re-quantization	[19]
Biorthogonal	3	Low	JND	$\langle 1, 0, 0, 0 \rangle (b = 1)$	[22]
Biorthogonal	3	All	Threshold	$\langle 1, 0, 0, 0 \rangle (b = 1)$	[23]
Biorthogonal	3	All	Threshold	$\langle 1, 0, 0, 0 \rangle (b = 1)$	[24]
Biorthogonal	5	All	All	$\langle 1, 0, 0, 0 \rangle (b = 1)$	[25]
Biorthogonal	5	All	Median	Intra Re-quantization	[26]
Biorthogonal	5	High	Threshold	$\langle 0, 1, 0, 0 \rangle$	[28]

**Fig. 5** Framework modules and input/output parameter blocks

4 Analysis framework

The analysis framework consists of three main functional modules: 1) Watermark embedding; 2) Scalable coding-based content adaptation; and 3) Watermark extraction and authentication. The high-level block diagram of the framework with main modular input/output parameters is shown in Fig. 5.

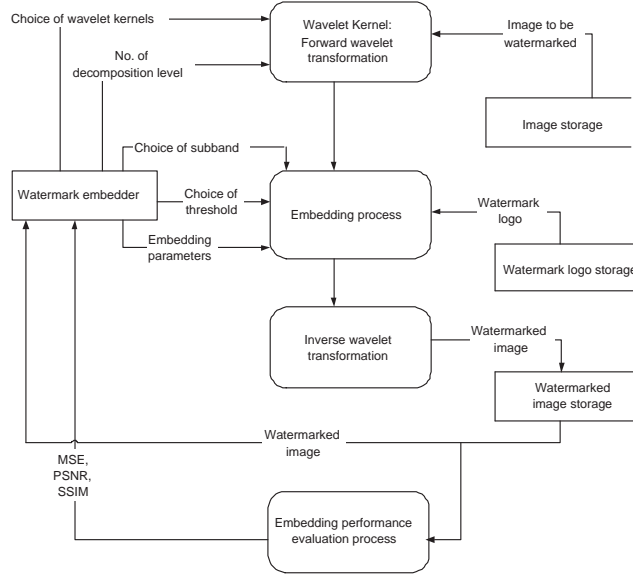


Fig. 6 Flow diagram of the watermark embedding module.

4.1 Watermark embedding module

Following the dissection of wavelet-based watermarking shown in Sect. 3, the watermark embedding module facilitates a common framework consisting of a tool repository for implementing those wavelet-based watermarking algorithms. The block diagram of the watermark embedding module consisting all input parameters, the sub module functional blocks, embedding performance evaluation, output parameters and their interconnected flow is shown in Fig. 6. The sub modules include the FDWT, watermark embedding, the IDWT, image display and embedding performance evaluation.

The input parameters to this module are three fold: operational; systems-related; and user-defined. Operational inputs are the host image and the watermark logo. The systems-related input parameters are related to the tools repository and consist of wavelet kernel choices, number of wavelet decomposition levels, host subband choice, host coefficient selection method and embedding procedure choice. The user-defined input parameters include embedding parameters, such as, thresholds, watermark strengths, and etc. The output parameters include the watermarked image and embedding performance evaluation metrics, such as, Mean Square Error (MSE), the Peak Signal to Noise Ratio (PSNR), Structural Similarity Measure (SSIM) and the data hiding capacity.

The FDWT submodule with its choices for the wavelet kernel is shown in Fig. 7. The currently available choices include orthogonal wavelets (Haar and Daubechies orthogonal), lifting-based [38] wavelets biorthogonal wavelets (9/7 and 5/3), separable non-linear wavelets [39, 40] and Quincunx sampling-based non-linear wavelets [39, 41]. For a flexible experimental environment the framework facilitates choosing any single or a group of subbands as the host subbands, fol-

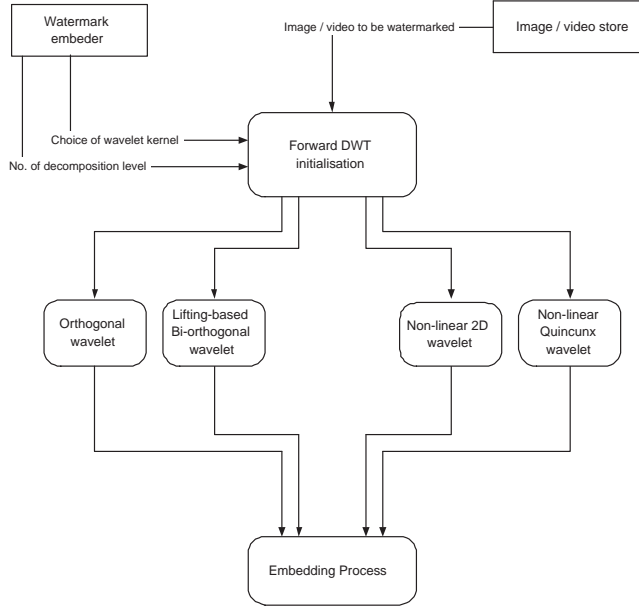


Fig. 7 The FDWT submodule with choices wavelet kernels.

lowed by coefficient selection based on the realization of the embedding methods discussed in Sect. 3.

4.2 JPEG2000 content adaptation module

Content adaptation module emulates of a heterogenous communication system, where the content is encoded using the JPEG2000 scalable coders to produce scalable bit streams. Such content may be adapted to address the varying network bandwidths, quality of services, display resolutions and usage requirements at various nodes of the network. These bit streams are adapted in terms of reducing quality, spatial resolutions and frame rates just by truncating various layers of the bitstream, resulting in low data rates to be streamed. During the robustness evaluation this module generates test images based on various bit rate of resolution scaling criteria.

4.3 Watermark extraction and authentication module

This module, extracts the watermark from the test images and authenticate the extracted watermark to evaluate the robustness. However a preprocessing step has been included to address the resolution scalability issue.

4.3.1 Watermark Extraction

The watermark extraction process can be either blind or non-blind depending on the coefficient selection and modification process used in the embedding algorithm.

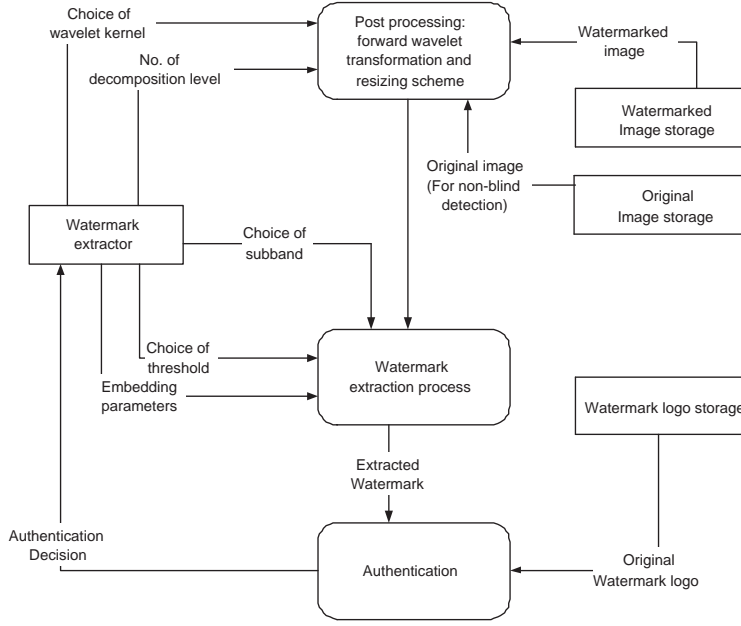


Fig. 8 Flow diagram of watermark extraction and authentication module.

In this framework, the schemes associated with magnitude alteration algorithms are non-blind, whereas, re-quantisation-based modifications are blind. In general, watermark extraction (as shown in Fig. 8) includes the FDWT followed by the finding of $\Delta_{m,n}$ either as $C'_{m,n} - C_{m,n}$ from Eq. (1) or as $f(\gamma, C_{min}, C_{max})$ from Eq. (3) to find the watermark information $W_{m,n}$.

Preprocessing: In the case of resolution scalability-based content adaptation, the resolution of the image of the decoded image is smaller than the original image and the watermarking synchronization is lost. To address such issue, we perform a preprocessing resizing scheme for the scaled test images. The resizing scheme follows three steps. Firstly, the decoded image is decomposed into $(N - M)$ levels using the FDWT employed in the compression algorithm, where N is the number of wavelet decomposition levels used in the embedding algorithm and M is the number of levels discarded due to content adaptation. Secondly, the normalization of all coefficients are adjusted by multiplying with 2^M . Finally the dimensions are extended to those of the original by zero padding the current matrix and the IDWT is applied to obtain the full resolution image.

4.3.2 Watermark Authentication

The authentication process verifies the extracted watermark with the original watermark. Two commonly used authentication metrics are Hamming Distance (H) (often referred as Bit Error Rate (BER)) and correlation similarity measure (S). The former is widely used for a binary watermark detection while the latter is commonly used for pseudo-random sequence-based watermark data or for a gray scale logo [14, 23]. Using these metrics, a watermark is said to be detected if the

Hamming Distance is lower than a threshold value or the correlation similarity measure is higher than a given threshold. These metrics are computed as follows:

$$H(W, W') = \frac{1}{L} \sum_{i=0}^{L-1} W_i \oplus W'_i, \quad (4)$$

$$\begin{aligned} S(W, W') &= \frac{W \cdot W'}{\sqrt{W' \cdot W'}} / \frac{W \cdot W}{\sqrt{W \cdot W}} \times 100, \\ &= \frac{W \cdot W'}{\sqrt{W' \cdot W'} \sqrt{W \cdot W}} \times 100, \end{aligned} \quad (5)$$

where W and W' are the original and the extracted watermarks, respectively. L is the length of the sequence and \oplus represents the *XOR* operation between the respective bits.

5 Evaluation results and discussion

In the section we use the proposed framework to evaluate the robustness of the watermarking techniques against the MPEG-21 DIA attacks, such as, JPEG2000-based quality scalable adaptations and JPEG2000-based resolution scalable adaptations.

5.1 The experimental setup

For these experiments, we use the first 100 images from INRIA natural holiday image data set [42] and binary logo as the watermark data. The PSNR is used for setting the host image distortion level to an acceptable level for embedding a given amount of watermarking data for robustness evaluation experiments. The Hamming distance (BER) is used as the authentication measure. The results show the mean value of the Hamming distance for the test image set and the error bars corresponding to 95% confidence level. The robustness against different compression ratios for the quality scalability attacks on the full resolution and joint resolution-quality scalability attacks (on half resolution) is evaluated. However, we have also conducted experiments to understand the effect on robustness evaluation on choosing different binary logo (varied distribution) as watermark; or how various embedding performance metric, *e.g.*, PSNR or SSIM behaves; or how the authentication metric *i.e.*, Hamming distance can be interpreted.

5.1.1 On the choice of logo

The experimental observations show that the choice of logo or a random sequence has no effect on the robustness performance of a given watermarking algorithm. As an example, we have used five different logo (as shown in Fig. 9) and evaluated the robustness performance. Fig. 10 shows the robustness performance for re-quantization based watermarking algorithm. The result indicates that irrespective of the used watermark logo, the trend of robustness under different resolution-quality scalability attacks remains the same. Considering such fact, in this work we have performed experiments in the following evaluations using only one logo.



Fig. 9 Test binary logo.

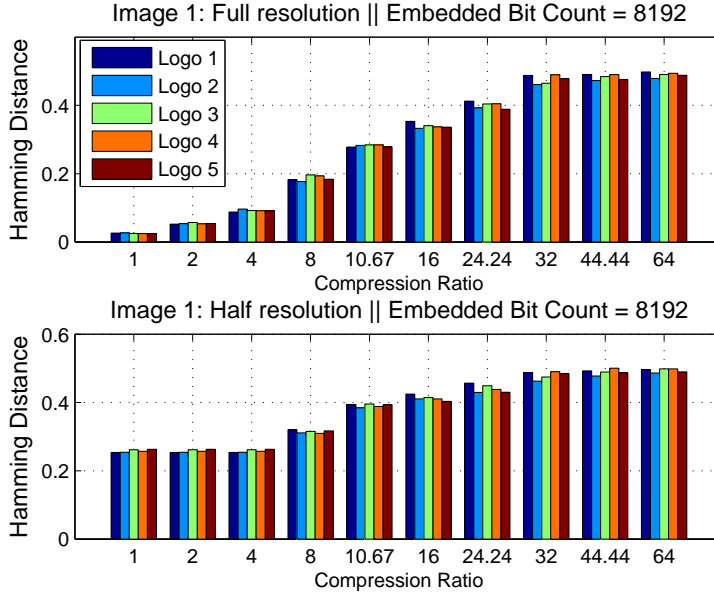


Fig. 10 An example of comparing the choice of logo with the same bit count (8192) being embedded using the intra re-quantization-based embedding on robustness to - *Row 1*: Quality scalability attack on full resolution; and *Row 2*: Joint resolution-quality scalability attack (half resolution).

5.1.2 On the use of PSNR in evaluations

In these experiments, the embedding performance is measured using the PSNR against data capacity. In robustness evaluation tests, we use this measures to ensure that either the distortion or data capacity is maintained constant for different watermarking algorithms, so that a fair comparison can be made for robustness under different embedding scenarios. Our initial experiments suggest that for most host images, if the PSNR is greater than 35dB, other objective measures, such as, weighted PSNR (wPSNR) and structural similarity index (SSIM), are highly correlated with the PSNR values. Therefore in the subsequent experiments we have used PSNR to evaluate the robustness keeping PSNR more than 35dB.

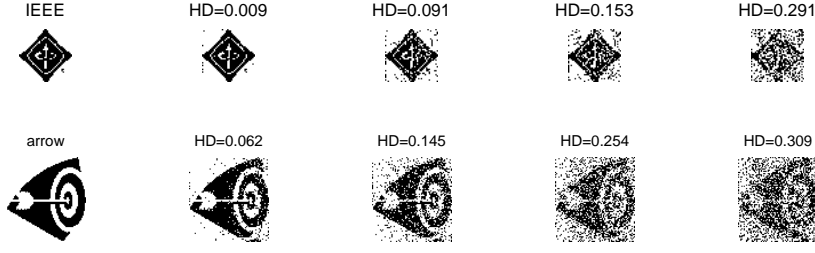


Fig. 11 Original and extracted watermark logo and corresponding to different Hamming distances (HD).

5.1.3 Hamming distance interpretation

The Hamming distance (BER) is used here as the authentication measure for robustness evaluation. Fig. 11 shows the visual quality corresponding to different Hamming distance values. The Hamming distances, calculated here, have been derived from the extracted watermark at various JPEG2000 compression rate. The logos corresponding to various Hamming distance are the reconstruction of the same extracted watermark bits. It is evident from these figures that after about 0.3 Hamming distance, the visual quality of logos become poor and become difficult to compare with the original logo. Based on the visual significance, one can define a threshold value of the Hamming distance to ensure the extracted watermark is visually comparable with the original logo. Based on our experiments a generalized hard threshold of 0.20 ± 0.02 and soft threshold up to 0.3 hamming distance can be set.

5.2 Robustness evaluation

Using the above discussed experimental set up, we considered three different scenarios to compare and evaluate the robustness against content adaptation. This is carried out by setting all but one parameters setting as common and fixed choices. For a fair robustness evaluation of various experimental set up, we have dynamically tuned the watermark strength parameter, α and γ , to achieve a tight bound of the PSNR, set to $37 \pm 0.5dB$ for every single test image. The scenarios, we considered are as follows:

5.2.1 The effect of wavelet kernel choice (Fig. 12 and Fig. 13)

We evaluate the contribution of the choice of wavelet kernel on the robustness to content adaptation by considering non-blind and blind extraction algorithms. The other parameters, namely, decomposition levels, the embedding subband and the host coefficient selection are set to three, low frequency and thresholds-based ($\langle 1, 0, 0 \rangle$ ($b=1$)) for the non-blind case and intra re-quantisation-based for the blind algorithm, respectively. A set of six different wavelet kernels representing three different wavelet classes, namely, orthonormal (Haar and D-4), bi-orthogonal

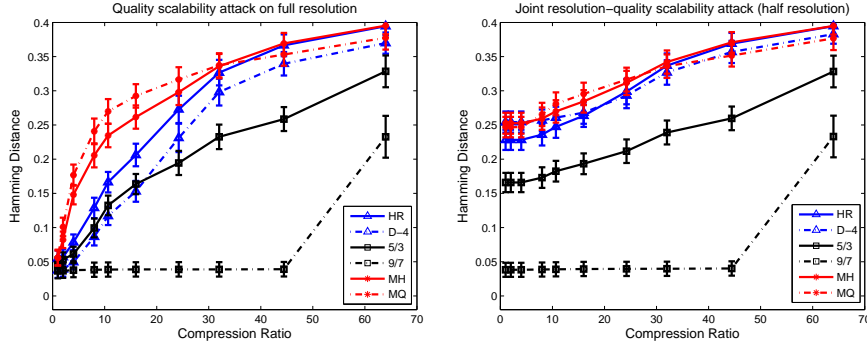


Fig. 12 On evaluating the effect of the wavelet kernel for $\langle 1, 0, 0, 0 \rangle$ ($b = 1$) direct modification-based embedding on robustness to - *Column 1*: Quality scalability attack on full resolution; and *Column 2*: Joint resolution-quality scalability attack (half resolution).

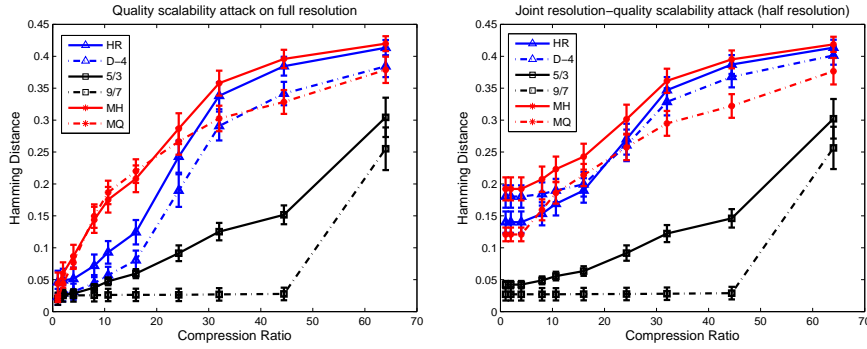


Fig. 13 On evaluating the effect of the wavelet kernel for intra re-quantization-based embedding on robustness to - *Column 1*: Quality scalability attack on full resolution; and *Column 2*: Joint resolution-quality scalability attack (half resolution).

(5/3 and 9/7) and non-linear (Morphological Haar and MQ) have been used for the comparisons. The results are shown in Fig. 12 (for the non-blind algorithm) and Fig. 13) (for the blind algorithm).

For the full resolution quality scalability as well as joint resolution-quality scalability attacks, the longer bi-orthogonal wavelets performed better compared to other wavelet kernels. Particularly bi-orthogonal 9/7 wavelet which is also used in JPEG2000 compression here, provides best result due to close approximation between watermarking wavelet and compression wavelet kernels. On the other hand, embedding performance varies for various wavelets due to variation in noise energy transfer for various wavelet kernel. Such a study has been proposed in [37]. This enables us to optimize the coefficient selection procedure which can have a trade off tradeoff between the embedding distortion and the robustness.

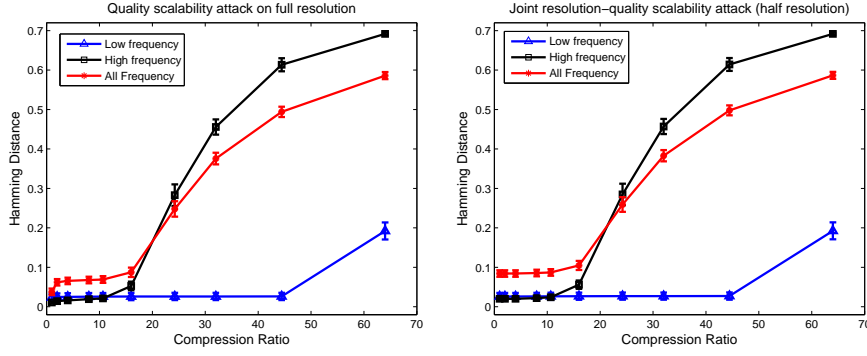


Fig. 14 On evaluating the effect of the subband choice for $\langle 1, 0, 0, 0 \rangle$ ($b = 1$) direct modification-based embedding on robustness to - *Column 1*: Quality scalability attack on full resolution; and *Column 2*: Joint resolution-quality scalability attack (half resolution).

5.2.2 The effect of subband choice (Fig. 14 and Fig. 15)

We compare the contribution of the choice of subbands for the robustness of a watermarking algorithm by setting all other choices to fixed. In this set of experiments, the wavelet kernel and decomposition levels are set to Haar and three, respectively. Fig. 14 shows the robustness performance for non-blind extraction that uses threshold-based ($\langle 1, 0, 0, 0 \rangle$ ($b=1$)) embedding method, while Fig. 15 shows the robustness performance for blind extraction that uses intra re-quantisation-based embedding. In plots, low, high and all frequency subband selection refers to the lowest frequency subband, three high frequency subbands in the third decomposition level and all four frequency subband in the third decomposition level, respectively.

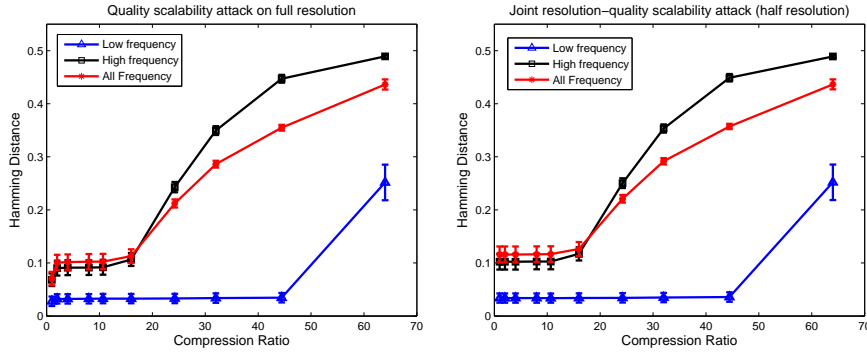


Fig. 15 On evaluating the effect of the subband choice for intra re-quantization-based embedding on robustness to - *Column 1*: Quality scalability attack on full resolution; and *Column 2*: Joint resolution-quality scalability attack (half resolution).

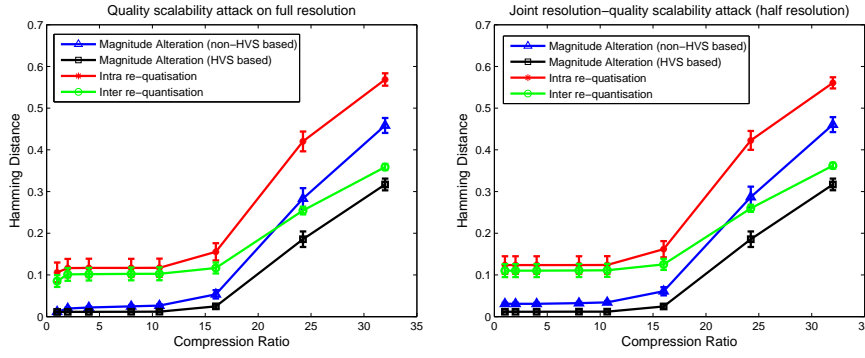


Fig. 16 On evaluating the effect of different embedding methods on robustness to - *Column 1*: Quality scalability attack on full resolution; and *Column 2*: Joint resolution-quality scalability attack (half resolution).

In both cases, embedding in low frequency subbands results in the highest robustness, compared to other two choices. This is mainly due to the high energy concentration in low frequency subband of the host image and the content scalability treatments used in JPEG2000 quality scalability and resolution scalability.

5.2.3 The effect of the choice of embedding method and host coefficient selection (Fig. 16)

In this experiment set, we have considered two different embedding methods, namely, magnitude alteration and re-quantization. For magnitude alteration, we considered two cases: HVS-based and all coefficient selection. For re-quantization-based methods we considered two cases: inter and intra subband coefficient selection. Other parameters, the wavelet kernel, decomposition levels and the embedding subband are set to Haar, three and high frequency subbands in the third decomposition level, respectively. It is evident from Fig. 16, for all different content adaptation scenarios, the HVS-based direct modification combination shows the highest robustness. This is mainly due to the efficiency in the coefficient selection method, enabling to choose a higher value for the watermark strength parameter, yet resulting in distortion performance in the specified range. Additionally a choice of coefficients in high frequency subbands can be robust to compression [34, 43] while providing higher imperceptibility. However, at a higher compression ratio, BER values (Hamming distance) of high frequency based watermarking schemes (refer to Fig. 14 and Fig. 16) are observed to be much larger (close to 0.7). This is due to heavy quantization process at higher compression ratios, leading to the loss of coefficient values in high frequency subbands. Therefore a tradeoff must be considered based on the application need.

6 Conclusions

Due to the emergence of JPEG2000 image coding standard, many wavelet based image watermarking techniques, robust to JPEG2000 compression, have been pro-

posed in the literature. We have categorized and evaluated the performances of such algorithms under a common framework to achieve three objectives of this paper. Firstly, we dissected different algorithms into common functional submodules, e.g., wavelet kernel, subband, host coefficient and embedding method. A new framework was then designed using these submodules to analyze the effects of various algorithmic parameters. Finally, a robustness evaluation against JPEG2000 content adaptation was performed using various combinations of the new framework. Such an evaluation helps the reader to understand the influence of these parametric choices to design a new optimized algorithm. For example, bi-orthogonal wavelet kernels (9/7 and 5/3 both) offered a better robustness while HVS based magnitude alteration method shows superiority compared other methods. Therefore, this may lead to further investigation into various bi-orthogonal wavelet kernel choice or devising strategy onto algorithmic design similar to HVS method. Further research in filter design for wavelet kernel may help to find highly imperceptible but robust watermarking solutions. The framework will also help to understand other future research directions in this domain, such as, a new embedding distortion metric (as PSNR or wPSNR does not necessarily reflect the embedding distortion measure required in watermarking perspective), or a unified robustness measurement metric which includes different parameters.

Acknowledgement

The sponsorship of the UK Engineering and Physical Sciences Research Council (EPSRC) by an EPSRC-BP (British Petroleum) Dorothy Hodgkin Postgraduate Award (DHPA) for this work is acknowledged.

References

1. D. S. Taubman and M. W. Marcellin, *JPEG2000 Image Compression Fundamentals, Standards and Practice*. USA: Springer, 2002.
2. H. Schwarz, D. Marpe, and T. Wiegand, "Overview of the scalable video coding extension of the H.264/AVC standard," *IEEE Trans. Circ. and Syst. for Video Tech.*, vol. 17, no. 9, pp. 1103–1120, Sept. 2007.
3. S. Kandadaï and C. D. Creusere, "Scalable audio compression at low bitrates," *IEEE Trans. Audio, Speech, and Language Processing*, vol. 16, no. 5, pp. 969–979, July 2008.
4. I. Burnett, R. V. de Walle, K. Hill, J. Bormans, and F. Pereira, "MPEG-21: goals and achievements," *IEEE Multimedia*, vol. 10, no. 4, pp. 60–70, Oct.-Dec. 2003.
5. A. Vetro, "MPEG-21 digital item adaptation: enabling universal multimedia access," *IEEE Multimedia*, vol. 11, no. 1, pp. 84–87, Jan.-March 2004.
6. L. Xie and G. R. Arce, "Joint wavelet compression and authentication watermarking," in *Proc. IEEE ICIP*, vol. 2, 1998, pp. 427–431.
7. F. Huo and X. Gao, "A wavelet based image watermarking scheme," in *Proc. IEEE ICIP*, 2006, pp. 2573–2576.
8. H. Tao, J. Liu, and J. Tian, "Digital watermarking technique based on integer Harr transforms and visual properties," in *Proc. SPIE Image Compression and Encryption Tech.*, vol. 4551-1, 2001, pp. 239–244.
9. X. Xia, C. G. Boncelet, and G. R. Arce, "Wavelet transform based watermark for digital images," *Optic Express*, vol. 3, no. 12, pp. 497–511, Dec. 1998.
10. G. Al-Hudhud, "Adaptation of HVS Sensitivity for Perceptual Modelling of Wavelet-Based Image Compression," in *Proc. Second Int'l Conf. in Visualisation*, 2009, pp. 196–200.
11. X. C. Feng and Y. Yang, "A new watermarking method based on DWT," in *Proc. Int'l Conf. on Computational Intelligence and Security, Lect. Notes in Comp. Sci. (LNCS)*, vol. 3802, 2005, pp. 1122–1126.

12. Q. Gong and H. Shen, "Toward blind logo watermarking in JPEG-compressed images," in *Proc. Int'l Conf. on Parallel and Distributed Comp., Appl. and Tech., (PDCAT)*, 2005, pp. 1058–1062.
13. M. Barni, F. Bartolini, and A. Piva, "Improved wavelet-based watermarking through pixel-wise masking," *IEEE Trans. Image Processing*, vol. 10, no. 5, pp. 783–791, May 2001.
14. D. Kundur and D. Hatzinakos, "Toward robust logo watermarking using multiresolution image fusion principles," *IEEE Trans. Multimedia*, vol. 6, no. 1, pp. 185–198, Feb. 2004.
15. G. Bhatnagar and Q.M. J. Wu and B. Raman, "Robust gray-scale logo watermarking in wavelet domain," *Computers & Electrical Engineering*, 2012.
16. M. R. Soheili, "Blind Wavelet Based Logo Watermarking Resisting to Cropping," in *Proc. 20th International Conference on Pattern Recognition*, 2010, pp. 1449–1452.
17. D. Kundur and D. Hatzinakos, "Digital watermarking using multiresolution wavelet decomposition," in *Proc. IEEE ICASSP*, vol. 5, 1998, pp. 2969–2972.
18. P. Campisi, A. Neri, and M. Visconti, "Wavelet-based method for high-frequency subband watermark embedding," in *Proc. SPIE Multimedia Sys. and Appl. III*, vol. 4209, 2001, pp. 344–353.
19. C. Jin and J. Peng, "A robust wavelet-based blind digital watermarking algorithm," *Information Technology Journal*, vol. 5, no. 2, pp. 358–363, 2006.
20. P. Meerwald and A. Uhl, "A survey of wavelet-domain watermarking algorithms," in *Proc. SPIE Security and Watermarking of Multimedia Contents III*, vol. 4314, 2001, pp. 505–516.
21. C.-Y. Yang, W.-Y. Hwang, and Y.-F. Cheng, "IWT-Based Watermarking By Adaptive Bit-Labeling Scheme," in *Proc Int'l Conf. on Intelligent Information Hiding and Multimedia Signal Processing*, 2008, pp. 1165–1168.
22. Z. Zhang and Y. L. Mo, "Embedding strategy of image watermarking in wavelet transform domain," in *Proc. SPIE Image Compression and Encryption Tech.*, vol. 4551-1, 2001, pp. 127–131.
23. J. R. Kim and Y. S. Moon, "A robust wavelet-based digital watermarking using level-adaptive thresholding," in *Proc. IEEE ICIP*, vol. 2, 1999, pp. 226–230.
24. S. Marusic, D. B. H. Tay, G. Deng, and P. Marimuthu, "A study of biorthogonal wavelets in digital watermarking," in *Proc. IEEE ICIP*, vol. 3, Sept. 2003, pp. II-463–6.
25. T.-S. Chen, J. Chen, and J.-G. Chen, "A simple and efficient watermarking technique based on JPEG2000 codec," in *Proc. Int'l Symp. on Multimedia Software Eng.*, 2003, pp. 80–87.
26. P. Meerwald, "Quantization watermarking in the JPEG2000 coding pipeline," in *Proc. Int'l Working Conf. on Comms. and Multimedia Security*, 2001, pp. 69–79.
27. Q. Sun and S. Chang, "A secure and robust digital signature scheme for JPEG2000 image authentication," *IEEE Trans. Multimedia*, vol. 7, no. 3, pp. 480–494, June 2005.
28. F. Dufaux, S. J. Wee, J. G. Apostolopoulos, and T. Ebrahimi, "JPSEC for secure imaging in JPEG2000," in *Proc. SPIE Appl. of Digital Image Processing XXVII*, vol. 5558-1, 2004, pp. 319–330.
29. L. Chunhua and F. Li, "Adaptive image watermarking algorithm based on biorthogonal wavelet transform," in *Proc Int'l Conf. on E-Business and E-Government (ICEE)*, 2011, pp. 1–4.
30. R. Grosbois, P. Gerbelot, and T. Ebrahimi, "Authentication and access control in the JPEG2000 compressed domain," in *Proc. SPIE Appl. of Digital Image Processing XXIV*, vol. 4472-1, 2001, pp. 95–104.
31. Y.-S. Seo, M.-S. Kim, H.-J. Park, H.-Y. Jung, H.-Y. Chung, Y. Huh, and J.-D. Lee, "A secure watermarking for JPEG2000," in *Proc. IEEE ICIP*, vol. 2, 2001, pp. 530–533.
32. M. A. Suhail, M. S. Obaidat, S. S. Ipson, and B. Sadoun, "A comparative study of digital watermarking in JPEG and JPEG2000 environments," *Information Sciences*, vol. 151, pp. 93–105, 2003.
33. D. Bhowmik and C. Abhayaratne, "Morphological wavelet domain image watermarking," in *Proc. European Signal Processing Conference (EUSIPCO)*, 2007, pp. 2539–2543.
34. C. Abhayaratne and D. Bhowmik, "Scalable watermark extraction for real-time authentication of JPEG2000 images," *Journal of Real-Time Image Processing*, vol. 6, no. 4, p. 19 pages, 2011.
35. N. Sprljan, M. Mrak, G. C. K. Abhayaratne, and E. Izquierdo, "A scalable coding framework for efficient video adaptation," in *Proc. Int'l Workshop on Image Analysis for Multimedia Interactive Services (WIAMIS)*, 2005.

36. D. Bhowmik and C. Abhayaratne, "A generalised model for distortion performance analysis of wavelet based watermarking," in *Proc. Int'l Workshop on Digital Watermarking (IWDW '08), Lect. Notes in Comp. Sci. (LNCS)*, vol. 5450, 2008, pp. 363–378.
37. —, "Embedding distortion modeling for non-orthonormal wavelet based watermarking schemes," in *Proc. SPIE Wavelet App. in Industrial Processing VI*, vol. 7248, 2009, p. 72480K (12 Pages).
38. I. Daubechies and W. Sweldens, "Factoring wavelet transforms into lifting steps," *Journal of Fourier Anal. Appl.*, vol. 4, no. 3, pp. 245–267, 1998.
39. G. C. K. Abhayaratne and H. Heijmans, "A novel morphological subband decomposition scheme for 2D+t wavelet video coding," in *Proc. Int'l Symp. on Image and Signal Processing and Analysis*, vol. 1, 2003, pp. 239–244.
40. F. J. Hampson and J.-C. Pesquet, "A nonlinear subband decomposition with perfect reconstruction," in *Proc. IEEE ICASSP*, vol. 3, 1996, pp. 1523–1526.
41. H. Heijmans and J. Goutsias, "Nonlinear multiresolution signal decomposition schemes: Part II: Morphological wavelets," *IEEE Trans. Image Processing*, vol. 9, no. 11, pp. 1897–1913, Nov. 2000.
42. H. Jegou, M. Douze, and C. Schmid, "Hamming embedding and weak geometric consistency for large scale image search," in *Proc. 10th European Conference on Computer Vision: Part I (ECCV'08)*. Springer-Verlag, 2008, pp. 304–317.
43. D. Bhowmik and C. Abhayaratne, "The effect of quality scalable image compression on robust watermarking," in *Proc. Int'l Workshop on Digital Signal Processing*, 2009, pp. 1–8.